Effect of Silica and Carbon-reducing Agents on Ni and Ti iImpurities During Silicon Production

Hongmei Zhang
Kunming University of Science and Technology - Lianhua Campus: Kunming University of Science and Technology
Zhengjie Chen (czjkmust@126.com)
Kunming University of Science and Technology
Jianhua Wen
Kunming University of Science and Technology - Lianhua Campus: Kunming University of Science and Technology
Wenhui Ma
Kunming University of Science and Technology - Lianhua Campus: Kunming University of Science and Technology
Shijie Cao
Kunming University of Science and Technology - Lianhua Campus: Kunming University of Science and Technology

Research Article

Keywords: Organic silicon, Coal, Petroleum coke, Silica, Impurities

Posted Date: June 17th, 2021

DOI: https://doi.org/10.21203/rs.3.rs-600648/v1

Version of Record: A version of this preprint was published at Silicon on July 26th, 2021. See the published version at https://doi.org/10.1007/s12633-021-01287-x.

Abstract

The Ni and Ti contents of industrial silicon has a significantly affect the of organic silicon. On the basis of large specific production data, the chemical component of silica and the carbon-reducing agent effect of the Ni and Ti contents of silicon were investigated using statistical techniques. Two furnaces were also studied—an 8.5 MVA furnace and a 12.5 MVA furnace. The effects of TiO_2 and NiO impurities on the power consumption of both furnaces were also evaluated using the correlation of the TiO_2 and NiO impurities in raw materials with specific power consumption. The consumption of raw materials exhibited a high negative correlation with the TiO_2 and NiO impurities in industrial silicon, as determined by linear regression—that is, 82% < |r| < 99%. The influence of Ni on industrial silicon production was also stronger than that of Ti. With an increase in Ni, the power consumption of the 8.5 MWA furnace significantly decreased, whereas that of the 12.5 MWA furnace is increased. Adjusting the content of Ni content can reduce the power consumption of industrial silicon production in the large furnace.

1. Introduction

Organic silicon, the pillar of strategic emerging industries, exhibits superior performance and is widely used in construction [1, 2], electronics [3–5], transportation [6], energy [7–9], and household products [10]. It is typically structured with the Si-C bond (or the Si-O, Si-S, Si-N bond). Most organic silicon compounds are organic, polymers with -Si-O-Si- as the main chain. Organic silicon products chlorosilanes in the upstream products for organic silicon monomer and then used as raw material for processing production of silicone oil, silicone rubber, silicone resin, silane coupling agent four categories of downstream products. Among these products, the organic silicon monomer is mainly crushed and ground into silicon powder via silicon blocks,

silicon powder and methyl chloride are directly synthesized into methyl chlorosilane (MCS) under the action of copper-based catalyst [11–14]. A diagram of the organic silicon industry chain is presented in Fig. 1. However, the reaction during production is more complex, and the quality of silica powder directly affects the synthesis reaction. Gillot [15] examined the reaction of CuCl with silicon containing impurities, such as Al, Fe, Ca, and Ti. They found that the presence of Ti increased the rate of copper formation during CuCl reduction by silicide. However, Tamhankar [16] showed that the presence of large amounts of free copper (not bonded to silicon) hinders the main reaction, leading to the formation of highly chlorinated silanes. Gillot [17] also found that Al promoted the reaction between Cu_3Si and CuCl, Fe reduced the consumption rate of Cu_3Si, and the combined action of the two impurities resulted in the formation of more Cu-Si alloys. MCS was synthesized into a siloxane mixture (DMC + D4), which was then polymerized into polysiloxane. Polysiloxane is the main raw material of the downstream products of organic silicon, and its quality directly affects the quality of the downstream products. Therefore, the analysis of impurities in silicon powder plays a key role in the synthesis of organic silicon monomers and the quality of downstream products.

Silicon is produced by reacting carbonaceous material and silica at high temperatures in an electric arc furnace but with the production of different impurities [18, 19]. Owing to the difficulty of removing some metal oxides, the calculation of the standard Gibbs free energy of the oxidizing impurity reaction in silicon shows that TiO_2 does not undergo reduction reaction at temperatures in the 0–2000 ºC range but can form a metallic phase ($FeSi_2Ti$) with silicon, an inert phase. Studies have shown that Ti can accumulate in the reactor in the form of slag during MCS production. NiO is partly reduced at about 899 ºC; however, during MCS synthesis, Ni can prioritize the formation of methyl hydrodichlorosilane (monomethyl hydrogen). The iron-philic Ni easily forms a precipitated state with silicon. Ni in large amounts inhibits the production reaction of organic silicone and thus needs to be strictly controlled. Related research shows that impurities in silicon can be classified as beneficial and harmful with each part needs to control a certain amount of impurities, depending on the characteristics of organic silicon production process. The Non-ferrous Metal Industry Standard of the People's Republic of China (YS/T 1109–2016) limits the contents of major impurities in silicon powder for organic silicon; for instance, Ti content is not to exceed 0.5%, Ni content is limited to 0.015%, and silicon content has to be in the 99.184–99.724% range. Further, the national

standard for industrial silicon (GB/T 2881 – 2014) for the content of trace elements of silicon used in organic silicon and silicon for organic silicon belongs to chemical silicon. The high-precision grade contains Ni ≤ 100×10^{-6} and Ti ≤ 400×10^{-6}, and the general-precision grade contains Ni ≤ 150×10^{-6} and Ti ≤ 500×10^{-6}.

Several studies have been conducted on the influence of the quality of organic silicon which has been identified as a direct factor [20, 21]. However, the content and source of trace elements in silicon (such as Ti and Ni) have yet to be clarified, and the presence of a linear relationship between the two has yet to be determined. These inadequacies hinder the repeatability of the reaction and affect product yield, impeding development of organic silicon. Evaluation and analytical techniques concerning industrial silicon have been developed [22–27]. We previously used linear regression to determine the effects of coal, petroleum coke, and silica in different furnaces on the amount of major impurities in industrial silicon [28]. Numerous studies have been performed to measure the effects of major impurities (Fe, Al, and Ca) in silicon production on raw materials and energy; by contrast, no comprehensive research has been reported regarding the effects of other minor impurities (Ti, Ni, K, etc.) on energy consumption and raw materials.

Therefore, from the perspective of raw material and power consumption, the sources of Ti and Ni oxide impurities and their effect on each other are evaluated to provide a theoretical basis for obtaining silicon powders with desirable properties. In the current study, we investigate the relationship between the silicon produced in two submerged arc furnaces and the Ti and Ni oxide impurities in the feedstock to determine how the relationship between the two oxides affects energy and feedstock consumption in silicon production.

2. Raw Materials And Research Method

2.1 Raw materials

Petroleum coke and coal, which were used as reducing agents in the production of industrial silicon (Si > 99%), were sourced from Taiwan and Shanxi. The properties of each raw material are listed in Table 1 and Table 2. The TiO_2 content in coal was 0.025%, and the NiO content in petroleum coke was 0.033%. The electrode material is considered to be 100% carbon fixed, but its effect on silicon production is temporarily being ignored.

Table 1
Proximate analysis of raw materials for silicon production (wet basis)

Raw materials	Fixed carbon (%)	Volatiles (%)	Moisture (%)	Ash (%)
Soft coal	55.67	41.67	4.80	2.67
Petroleum coke	89.4	10.30	9.33	0.32

Table 2
Oxide contents of raw materials. (wt. %)

Raw materials	Fe_2O_3 (%)	Al_2O_3 (%)	CaO (%)	MgO (%)	P_2O_5 (%)	SO_3 (%)	TiO_2 (%)	NiO (%)	K_2O (%)	SiO_2 (%)	C (%)	Na_2O (%)
Soft coal	0.270	0.440			< 0.001	0.581	0.025	0.004	0.008	1.137	97.195	
Petroleum coke	0.047	0.046			< 0.001	9.528	0.002	0.033	< 0.001	0.966	89.258	
Silica	0.067	0.484	0.06	0.036	0.004	< 0.003	0.007		0.188	98.816		0.025

Figure 2 shows the consumption of different carbon materials and the electric energy required by the 8.5 MVA and 12.5 MVA furnaces. As shown in the figure, the power consumption of the 12.5 MVA furnace fluctuates but mostly stays between 1200 and 1400 kwh, whereas that of the 8.5 MVA furnaces is between 1200 and 1370 kwh. The coal consumption of the 12.5 MVA furnace is consistently higher than that of petroleum coke, whereas that of the 8.5 MVA furnace is the opposite.

2.2 Effect of the carbon-reducing agent on TiO_2/NiO impurity balance in industrial silicon production process

Impurities during smelting of industrial silicon mainly originate from raw materials. Figure 3 presents the flow histogram of the TiO_2 and NiO impurities from different raw materials in the 8.5 MVA and 12.5 MVA furnaces. As shown in the figure, the diversion of impurities by different combinations of furnace feedstock markedly varies. In the 8.5 MVA furnace, the proportions of the TiO_2 and NiO impurities were as follows: coal feedstock, 50.77%; petroleum coke, 37.97%; and silica, 11.26%. After a reduction in high temperature, the proportions of the impurities were 8.00% in industrial silicon, 4.00% in micro silicon powder, and 10.82% in silicon slag; the rest flowed to waste gas recovery and purification. The proportions of TiO_2 and NiO impurities in industrial silicon were 57% and 43%, respectively. In the 12.5 MVA furnace, the proportions of TiO_2 and NiO impurities were 31.79% in the coal feedstock and 57.07% in petroleum coke, whereas the proportion of the aforementioned impurities in silica was basically unchanged—that is, 7.70% in industrial silicon. Moreover, the proportions of impurities in the 12.5 MVA furnace were slightly lower than those in the 8.5 MVA furnace. The proportions of TiO_2 and NiO impurities in industrial silicon were 66% and 34%, respectively. In general, variations in the ratios of raw materials affect the content of impurities, and the large furnace was beneficial to silicon production.

Figure 2 shows that a certain amount of the TiO_2 and NiO impurities attributed to raw materials during the smelting of industrial silicon affects the smelting process of industrial silicon. To explore the sources of impurities in raw materials and ensure that the quality of industrial silicon products could meet the standards of organic silicon production, the sources of different contents of TiO_2 and NiO impurities in different furnace models were analyzed. Figure 4 shows that the sources of TiO_2 and NiO oxides in petroleum coke, coal, and silica during smelting of industrial silicon. In the 8.5 MVA furnace, the content of TiO_2 impurities in the raw materials, ranked in descending order, was as follows: coal > petroleum coke > silica. The impurities in coal fluctuated between 25% and 70%. Petroleum coke varied between 30% and 45%, and silica was about 10%; NiO in petroleum coke differed between 25% and 50%, and coal fluctuated between 40% and 70%. In the 12.5 MVA furnace, the content of TiO_2 impurities, ranked in descending order, was as follows: petroleum coke > coal > silica. The TiO_2 impurities in petroleum coke varied between 41% and 75%, and that in coal fluctuated ranged between 25% and 35%. NiO in petroleum coke fluctuated from 41–67%, and coal varied between 20% and 35%. Therefore, the results provide a reference for adjusting and controlling the contents of impurities in raw materials to address quality problems of industrial silicon products, improve the quality of silicon powder, and effectively reduce the cost.

2.3 Data collection

During analysis, continuous production data for the 8.5 MVA furnace and the 12.5 MVA furnace for more than three months were collected, and abnormal data caused by power outages and failures were deleted. All units of data are one ton.

2.4 Calculation method

To determine the correlation between raw material consumption and impurity content in industrial silicon, the Pearson correlation coefficient [29] was adopted, expressed in Formula (1). r is the linear correlation coefficient, between − 1 and + 1. When $|r| \geq 0.80$ is highly relevant, the following relations apply: $0.5 \leq |r| < 0.8$ for moderate correlation, $0.3 \leq |r| < 0.5$ for low correlation, and $|r| < 0.3$ considerably weak correlation.

$$r = \frac{\sigma^2_{x_i y_i}}{\sigma_{x_i}\sigma_{y_i}} = \frac{\frac{\sum (x_i - \bar{x}_i)(y_i - \bar{y}_i)}{n}}{\sqrt{\frac{\sum (x_i - \bar{x}_i)^2}{n} \times \sqrt{\frac{\sum (y_i - \bar{y}_i)^2}{n}}}} = \frac{\sum (x_i - \bar{x}_i)(y_i - \bar{y}_i)}{\sqrt{\sum (x_i - \bar{x}_i)^2} \times \sqrt{\sum (y_i - \bar{y}_i)^2}} \quad (1)$$

3. Results And Discussion

3.1 Influence of raw materials on the TiO_2 and NiO total impurity content of silicon

Figure 5 presents the linear fitting diagram of the TiO_2 and NiO impurities in silicon and raw materials. As shown in the figure, the content of impurities increases with an increase in raw materials. In the 8.5 MVA furnace, the correlation coefficients of coal, petroleum coke, and silica were 0.69031, 0.80469, and 0.80317, respectively, with corresponding slopes of 0.52, 0.43, and 0.13, respectively. In the 12.5 MVA furnace, the correlation coefficients of the raw materials were 0.64426, 0.75578, and 0.81092, respectively, with slopes of 0.34, 0.53, and 0.15. Coal was only moderately correlated, whereas petroleum coke was highly correlated, with the content of impurities in silicon. The coal in the 8.5 MVA furnace most strongly affected the content of impurities in silicon, followed by petroleum coke. In the 12.5 MVA furnace, petroleum coke exerted the strongest effect, followed by coal.

To elucidate the relation between the TiO_2 and NiO impurities and raw materials in industrial silicon, their linear relation and percentage of total impurities in raw materials are presented in Fig. 6. Raw materials consumption was negatively correlated with the amount of impurities in industrial silicon. In the 8.5 MVA furnace, the $|r|$ values of coal, petroleum coke, and silicon were 0.87407, 0.96507, and 0.98253, respectively. In the 12.5 MVA furnace, the $|r|$ values of coal, petroleum coke, and silicon were 0.83231, 0.81920, and 0.97312, respectively. $|r| \geq 0.80$ indicates a high negative correlation—that is, the content of impurities in industrial silicon decreases gradually with an increase in raw material consumption. The slopes of the equation of the line in the figure vary. In the 8.5 MVA furnace, the absolute values of the slopes of coal, petroleum coke, and silica were 0.45, 0.40, and 0.12, respectively, and those in the 12.5 MVA furnace were 0.17, 0.23, and 0.07 respectively. The comparison shows the absolute value of the slope of the raw material in the small furnace was greater than that of the raw material in the large furnace. This difference suggests that variations in furnace type influence the production of industrial silicon, but the influence of impurities in the large furnace is reduced.

3.2 Influence of raw materials on the content of TiO_2 impurities in silicon

To understand the correlation between the single impurity in silicon products and the impurities in raw materials, as well as provide theoretical guidance for the effect of the content of TiO_2 and NiO impurities in raw materials on the production process of industrial silicon, the linear fitting between TiO_2 and the raw material is presented in Fig. 7. In the 8.5 MVA the $|r|$ values of the coal, petroleum coke, and silica were 0.81408, 0.80599, 0.89291, indicating a high negative correlation. In the 12.5 MVA furnace, the $|r|$ values of coal and petroleum coke were 0.71674 and 0.73965, respectively, suggesting a moderate negative correlation; meanwhile, the $|r|$ value of silica was 0.80078, exhibiting a high negative correlation. The percentage of impurity decreased with an increase in raw material. A comparison of the slope values in the two furnace types revealed that the absolute slope values of coal, petroleum coke, and silicon in the 8.5 MVA furnace were 0.27, 0.20, and 0.06, respectively;

moreover, the order of the degree of influence on silicon impurities was coal > petroleum coke > silica. The TiO_2 impurities were primarily ascribed to coal. The absolute values of slope in the 12.5 MVA furnace were 0.09, 0.13, and 0.04, respectively; the order of the degree of influence on silicon impurities was petroleum coke > coal > silica. The TiO_2 impurities were mainly attributed to petroleum coke.

3.3 Influence of raw materials on the content of NiO impurities in silicon

The linear fitting between NiO and the raw material is depicted in Fig. 8. In the 8.5 MVA furnace, the $|r|$ value of coal was 0.74957, indicating a moderate negative correlation; the $|r|$ values of petroleum coke and silica were 0.84513 and 0.84061, respectively, indicating a high negative correlation. In the 12.5 MVA furnace, the $|r|$ values of coal, petroleum coke, and silicon were 0.66652, 0.60343, and 0.76129, suggesting a moderate negative correlation. In the 8.5 MVA furnace, the absolute values of the slope of the coal, petroleum coke, and silicon were 0.22, 0.18, and 0.05, respectively; the corresponding values in the 12.5 MVA furnace were 0.08, 0.0.09, and 0.03, respectively. These results show that the large furnace type exerted the least effect on the production of industrial silicon. In the small furnace, the NiO impurities mainly came from coal, whereas in the large furnace, the NiO impurities mainly originated from petroleum coke.

3.4 Linear fitting of the effect of TiO_2–NiO interaction in silicon

To understand the interaction between TiO_2 and NiO impurities in industrial silicon, a linear fitting diagram of TiO_2 and NiO impurities in the two furnace types of industrial silicon is presented in Fig. 9. In the 8.5 MVA furnace, the two exhibited a low positive correlation, indicating that specific TiO_2 does not considerably change with an alteration in NiO consumption, but a certain trend of change still exists. With an increase in NiO content, the TiO_2 content also increased; the r value was determined to be 0.28113, and the slope was 0.33. In the 12.5 MVA furnace, the two were positively correlated, with an r of 0.23751. This value is significantly lower than that for the 8.5 MVA furnace with a slope of 0.45. The slopes of the two furnaces were compared; that of the 12.5 MVA furnace was much higher than that of the 8.5 MVA furnace, indicating that the NiO content in the larger furnace significantly influenced the production process. Therefore, regulating the NiO content can reduce the effect on industrial silicon production.

3.5 Influence of variations in the combination of reductants on power consumption in industrial silicon production

3.5.1 Effect of TiO_2 and NiO metal oxides in raw materials on power consumption in industrial silicon production

To elucidate the influence of TiO_2 and NiO impurities on the production of industrial silicon, the linear relationship between the two metal oxides and power consumption is depicted in Fig. 10. The figure reveals a moderate positive correlation between metal oxides and power consumption; the power consumption increases with an increase in the content of impurities. In the 8.5 MVA furnace, the r of NiO was 0.58473, the slope was 24546; meanwhile, the r of TiO_2 was 0.53939, and the slope was 16732. For the two linear equations, when the same impurity Δx_1 was consumed, the effective growth of energy consumption Δy_1 corresponding to NiO was 874 kwh, and that corresponding to TiO_2 was 584 kwh. This result indicates that the NiO impurity substantially affected power consumption. In the 12.5 MVA furnace, the r of NiO was 0.62033, with a slope of 31989, and the r of TiO_2 was 0.69029, with a slope of 16014. When the two linear equations consumed the same impurity Δx_2, the effective growth of energy consumption Δy_2 corresponding to NiO was 1893 kwh, and that corresponding to TiO_2 was 1010 kwh. A comparison of the two furnace types revealed that the r of TiO_2 in the large furnace was larger but the slope was smaller than that in the small furnace, indicating that the influence of TiO_2 in the large furnace was smaller than that in the smaller furnace; meanwhile, the r and slope of NiO in the large furnace were significantly larger, indicating that the NiO impurity significantly affected the power consumption of the large furnace.

3.5.2 Influence of the interaction between two impurity oxides on power consumption in the 8.5 MVA furnace

The influence of the TiO_2–NiO interaction on power consumption was assessed by contour analysis, as shown in Fig. 11. The figure on the left is a three-dimensional stereogram, and the figure on the right is a two-dimensional contour map. As shown in the figure illustrating the 8.5 MVA furnace, with an increase in NiO impurity content, power consumption decreases gradually, and particularly when NiO > is 0.14 t, power consumption is significantly reduced. In the figure presenting the 12.5 MVA furnace, power consumption gradually increases with an increase in NiO content. Power consumption was at its highest provided that $TiO_2 \geq 0.2943$ t and $0.1885 \leq TiO_2 \leq 0.3361$ t. In summary, with an increase in Ni, the effect on power consumption in the small furnace decreased, whereas that on power consumption in the large furnace increased. Therefore, the production cost can be reduced to a large extent by adjusting the influence of reduction in Ni content on the production in the large furnace.

4. Conclusion

The effects of three raw materials in 8.5 MVA and 12.5 MVA ore furnaces on the Ti and Ni contents in industrial silicon were evaluated based on large-scale industrial data. Results indicate that the TiO_2 and NiO impurities and the raw material exhibited a high negative correlation—$82\% < |r| < 99\%$; the percentage of impurities decreased with an increase in raw material. The percentage of a single-element impurity exhibited a trend similar to that of the total impurities. The correlation coefficient $|r|$ of the TiO_2 in the 8.5 MVA furnace and coal was the largest—that is, 81.4%; the correlation coefficient $|r|$ of petroleum coke and NiO reached 84.5%. TiO_2 and petroleum coke in the 12.5 MVA furnace showed a correlation coefficient $|r|$ of 74.0%; NiO and coal had a correlation coefficient $|r|$ of 66.7%. The linear fit between TiO_2 and NiO in the 12.5 MVA furnace had a slope of 0.45, which was higher than the slope obtained in the 8 MVA furnace (0.33). Thus, compared with the TiO_2 content, the NiO content more strongly influenced industrial silicon production. Moreover, with an increase in NiO content, the power consumption in the small furnace decreased, whereas that in the large furnace increased. The Ti impurities exerted less influence on silicon production, compared with the Ni impurities. Thus, the quality of industrial silicon could be improved by adjusting the Ni content, and the production cost could be reduced. Further, the research results bear significance for improving the quality of organic silicon and the manufacture of the downstream products of organic silicon.

Declarations

Acknowledgments

The authors are grateful for financial support from the National Natural Science Foundation of China (No. 51804147) and the Yunnan Province Department of Education (No. 2018JS018).
Ethics approval and consent to participate We don't cover ethics approval and consent to participate. * Consent for publication Not applicable. * Availability of data and materials All data generated or analysed during this study are included in this published article. * Competing interests The authors declare that they have no competing interests. * Funding The authors are grateful for financial support from the National Natural Science Foundation of China (No. 51804147) and the Yunnan Province Department of Education (No. 2018JS018). * Authors' contributions Hongmei Zhang: Conceptualization, Resources, Writing - review & editing, Visualization, Validation, Supervision. Zhengjie Chen: Formal analysis, Validation, Data curation, Writing-original draft, Writing-review&editing. Jianhua Wen:Conceptualization, Methodology, Validation, Formal analysis, Investigation, Data curation. Wenhui Ma: Conceptualization, Resources, Visualization, Visualization, Supervision. Shijie Cao: Writing - review & editing. * Authors' information (optional) Hongmei Zhang1,2, Zhengjie Chen1,2,3*, Jianhua Wen1*, Wenhui Ma1,2,3, Shijie Cao1,2,3 1 Faculty of Metallurgical and Energy Engineering, Kunming University of Science and Technology, Kunming 650093, China; 2 State Key Laboratory of Complex Nonferrous Metal Resources Cleaning Utilization in Yunnan Province, Kunming University of Science and Technology, Kunming 650093, China; 3 The National Engineering Laboratory for Vacuum Metallurgy, Kunming University of Science and Technology, Kunming 650093, China; *Corresponding author: E-mail address: czjkmust@126.com (Z. Chen); qjmlwjh@163.com(J. Wen) * Disclosure of potential

conflicts of interest We declare that we have no conflict of interest. * Research involving Human Participants and/or Animals Not applicable. * Informed consent Not applicable

References

[1] Xiao, J.S., Lu, C.T., Jiang, S., Li, Y., 2020. Research and Application of Anticorrosive Coating for Reinforced Concrete of Coastal Buildings. Journal of Coastal Research, 103:417-421.

[2] Ma, M., Chen, Q., Wang, C., Fu, H., Li, T., 2019. High-performance organic silicon-refractory bauxite: Coating and fundamental properties. Construction and Building Materials, 207:563-571.

[3] Kim, H.K., Ryu, M.K., Kim, K.D., Lee, S.M., Cho, S.W., Park, J.W., 1998. Tunable Electroluminescence from Silicon-Containing Poly(p-phenylenevinylene)-Related Copolymers with Well-Defined Structures. Macromolecules, 31(4):1114-1123.

[4] Gong, S.L., Chen, Y.H., Yang, C.L., Zhong, C., Qin, J.G., Ma, D.G., 2010. De Novo Design of Silicon-Bridged Molecule Towards a Bipolar Host: All-Phosphor White Organic Light-Emitting Devices Exhibiting High Efficiency and Low Efficiency Roll-Off. Advanced Materials, 22(47):5370-5373.

[5] Hoffmann, F., Cornelius, M., Morell, J., Fröba, M., 2006. Periodic mesoporous organosilicas (PMOs): past, present, and future. J Nanosci Nanotechnol, 6(2):265-288.

[6] Jin, L., Zhang, X., Cui, C., Xi, Z., Sun, J., 2021. Simultaneous Process Parameters and Heat Integration Optimization for Industrial organic silicon Production. Separation and Purification Technology, 265(1):118520.

[7] Le, Y., Tabachnyk, M., Bayliss, S.L., Böhm, M.L., Broch, K., Greenham, N.C., Friend, R.H., Ehrler, B., 2015. Solution-Processable Singlet Fission Photovoltaic Devices. Nano Letters, 15(1).

[8] Kakiage, K., Aoyama, Y., Yano, T., Oya, K., Kyomen, T., Hanaya, M., 2015. Fabrication of a high-performance dye-sensitized solar cell with 12.8% conversion efficiency using organic silyl-anchor dyes. Chemical Communications, 51(29):6315-6317.

[9] Uekert, T., Solodovnyk, A., Ponomarenko, S., Osvet, A., Levchuk, I., Gast, J., Batentschuk, M., Forberich, K., Stern, E., Egelhaaf, H.-J., Brabec, C.J. 2016. Nanostructured organic silicon luminophores in highly efficient luminescent down-shifting layers for thin film photovoltaics. Solar Energy Materials and Solar Cells. 155:1-8.

[10] Horii, Y., Kannan, K., 2008. Survey of organic silicone Compounds, Including Cyclic and Linear Siloxanes, in Personal-Care and Household Products. Archives of Environmental Contamination & Toxicology, 55(4):701-710.

[11] Luo, W., Wang, G., Wang, J., 2006. Effect of CuCl particle size on the reduction reaction by silicon in preparation of contact mass used for methylchlorosilane synthesis. Industrial & Engineering Chemistry Research, 45(1):559-69.

[12] Seyferth, D., 2001. Dimethyldichlorosilane and the Direct Synthesis of Methylchlorosilanes. The Key to the Silicones Industry. Organometallics, 20(24):4978-4992.

[13] Wang, C., Wang, G., Wang, J., 2014. A Bi-component Cu Catalyst for the Direct Synthesis of Methylchlorosilane from Silicon and Methyl Chloride. Chinese Journal of Chemical Engineering, 22(3):299-304.

[14] Seyferth, D., 2001. Dimethyldichlorosilane and the Direct Synthesis of Methylchlorosilanes. The Key to the Silicones Industry. Organometallics, 20(24).

[15] Gillot, B., Souha, H., Viale, D., 1992. Kinetic study of the reaction between copper(I) chloride and commercial silicon or silicides. Journal of Materials Science, 27(5):1337-1342.

[16] Tamhankar, S.S., Gokarn, A.N., Doraiswamy, L.K., 1981. Studies in solid-solid reactions: Autocatalysis in the reduction of cuprous chloride by silicon. Chemical Engineering Science, 36(8):1365-1372.

[17] Gillot, B., Weber, G., Souha, H., Zenkouar, M., 1998. Reactivity of commercial silicon and silicides towards copper(I) chloride. Effect of aluminium, calcium and iron on the formation of copper silicide. Journal of Alloys & Compounds, 270(1):275-280.

[18] Xi, F.S., Li, S.Y., Ma, W.H., Chen, Z.J., Wei, K.X., Wu, J.J., 2021. A review of hydrometallurgy techniques for the removal of impurities from metallurgical-grade silicon. Hydrometallurgy, 201:105553.

[19] Chen, Z.J., Ma, W.H., Wu, J.J., Wei, K.X., Lei, Y., Lv, G.Q., 2017. A Study of the Performance of Submerged Arc Furnace Smelting of Industrial Silicon. Silicon, 10:1121-1127.

[20] Cui, Y., Zhao, Y.T., Cui, H., Cui, L., Li, B., 2010. Effect of the quality of silicon powder on the selectivity of methylchlorosilane. Journal of Jilin Institute of Chemical Technology.

[21] Jia, Y.Z., Zhou, C.Y., Zhang, G.H., 2007. The influence of the quality of silicon powder on synthesis of methylchlorosilanes. Silicone Material.

[22] Saevarsdottir, G., Hjartarson, H., Palsson, H., 2010. Waste heat utilization from a submerged arc furnace producing ferrosilicon. Proceedings of the 12th International Ferroalloys Congress: Sustainable Future

[23] Kamfjord, N.E., Myrhaug, E.H., Tveit, H., Wittgens, B., 2010. Energy balance of a 45 MW (ferro-) silicon submerged arc furnace. In: Proceedings of the Twelfth International Ferro Alloy Congress. Helsinki Finland 729-738.

[24] Takla, M., Kamfjord, N.E., Tveit, H., Kjelstrup, S, 2013. Energy and exergy analysis of the silicon production process. Energy, 58:138-146.

[25] Brset, M.T., Kolbeinsen, L., Tveit, H., Kjelstrup, S., 2015. Exergy based efficiency indicators for the silicon furnace. Energy, 90:1916-1921.

[26] Chen, Z.J., Ma, W.H., Li, S.Y., Wu, J.J., Wei, K.X., Tu, Z.Q., Ding, W.M., 2018. Influence of carbon material on the production process of different electric arc furnaces. Journal of Cleaner Production, 174:17-25.

[27] Chen, Z.J., Zhou, S.C., Ma, W.H., Deng, X.C., Li, S.Y., Ding, W.M., 2018. The effect of the carbonaceous materials properties on the energy consumption of silicon production in the submerged arc furnace. Journal of Cleaner Production, 191:240-247.

[28] Zhang, H.M., Chen, Z.J., Ma, W.H., Cao, S.J., Jiang, K.Z., Zhu, Y.Q., 2021. The Effect of Silica and Reducing Agent on the Contents of Impurities in Silicon Produced. Silicon, 1-14.

[29] Eberly, L.E., 2003. Correlation and Simple Linear Regression. Radiology, 227(3):617-622.

Figures

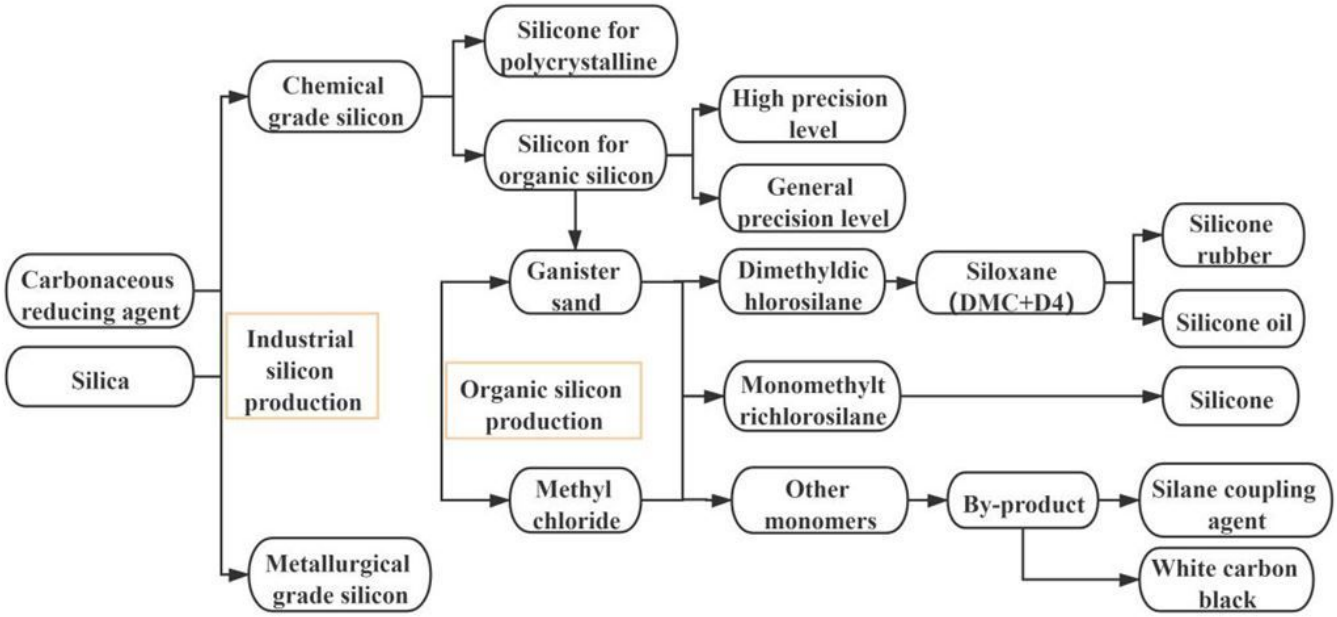

Figure 1

Organic silicon industry chain map

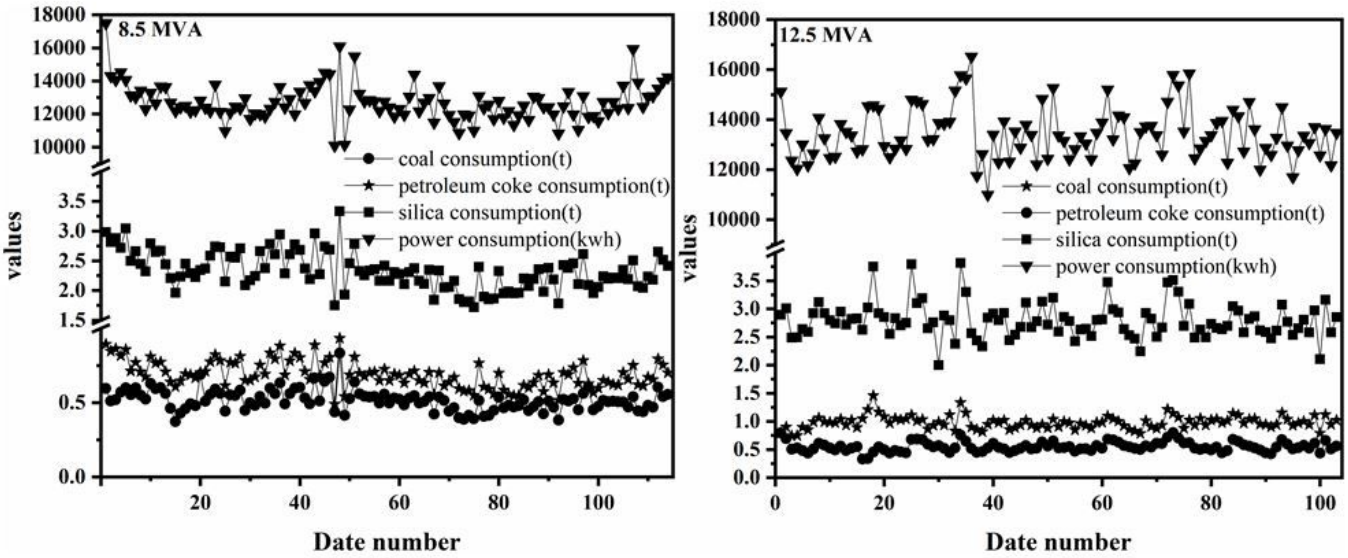

Figure 2

Carbon material and electricity consumption

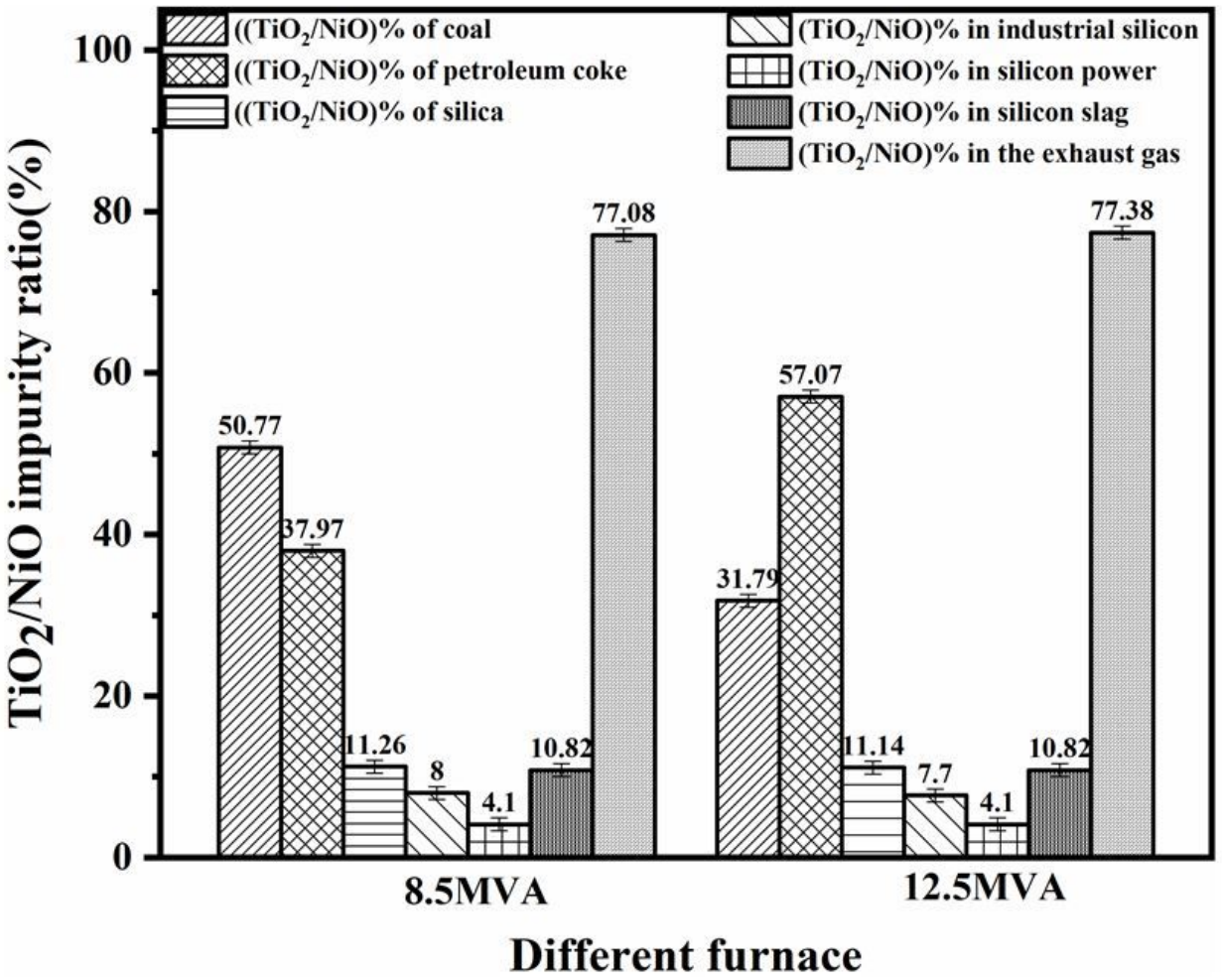

Figure 3

Histogram of raw material in impurity input and output during silicon production

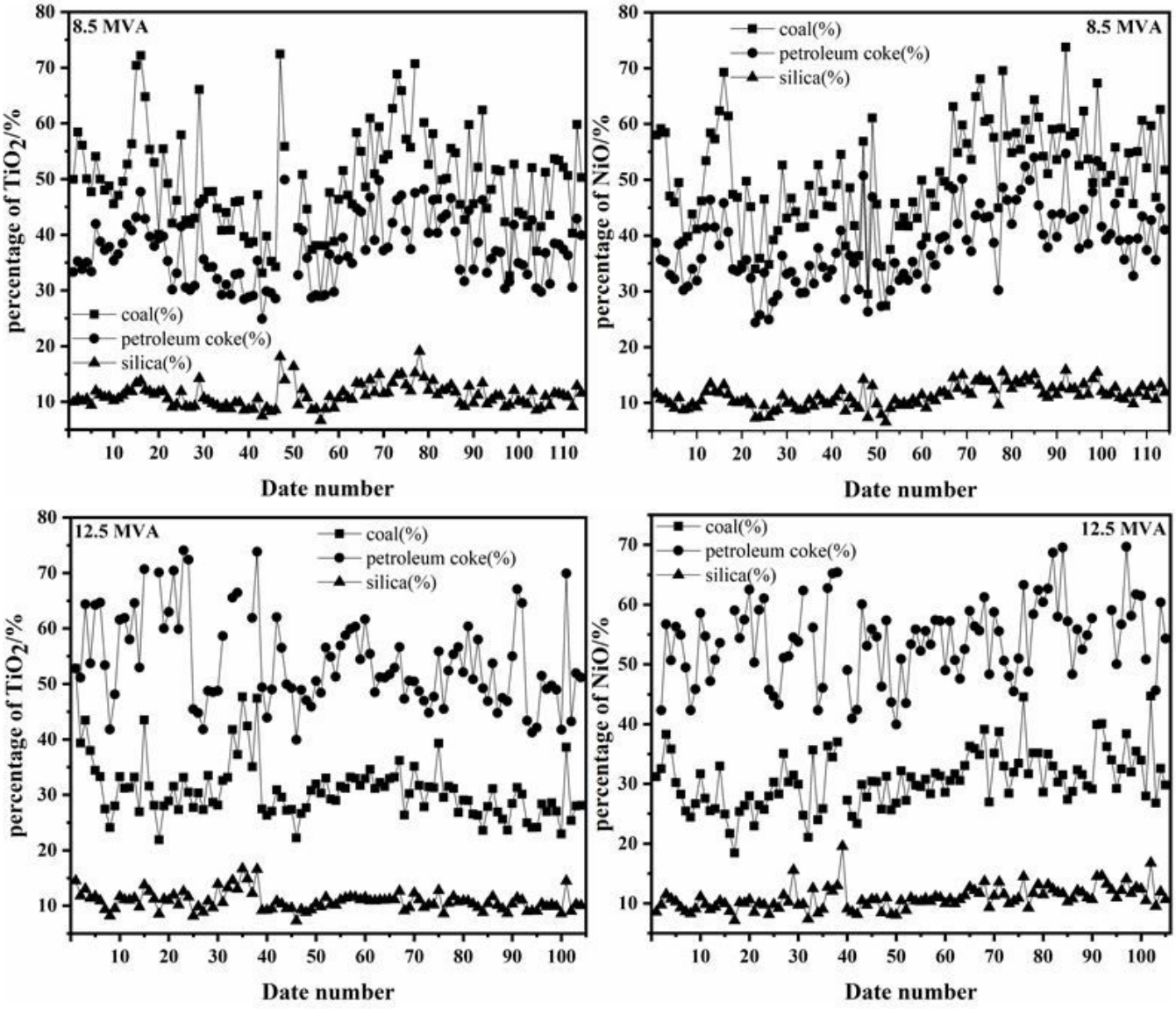

Figure 4

Sources of TiO2 and NiO impurity oxides in industrial silicon smelting process

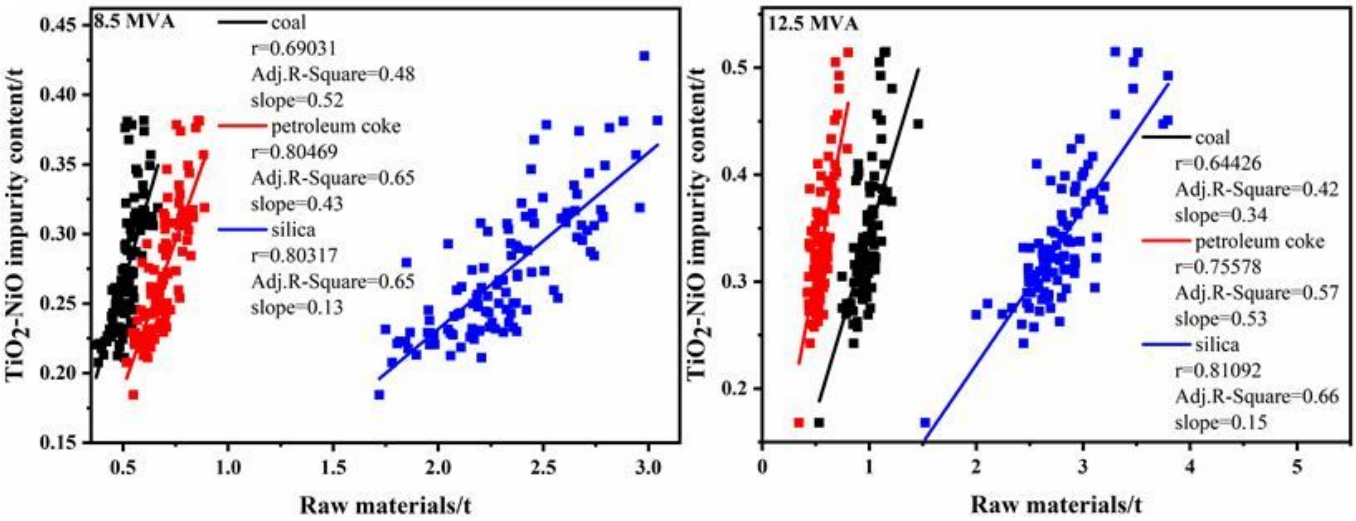

Figure 5

Linear fitting relationship between TiO2/NiO impurity in silicon and raw material

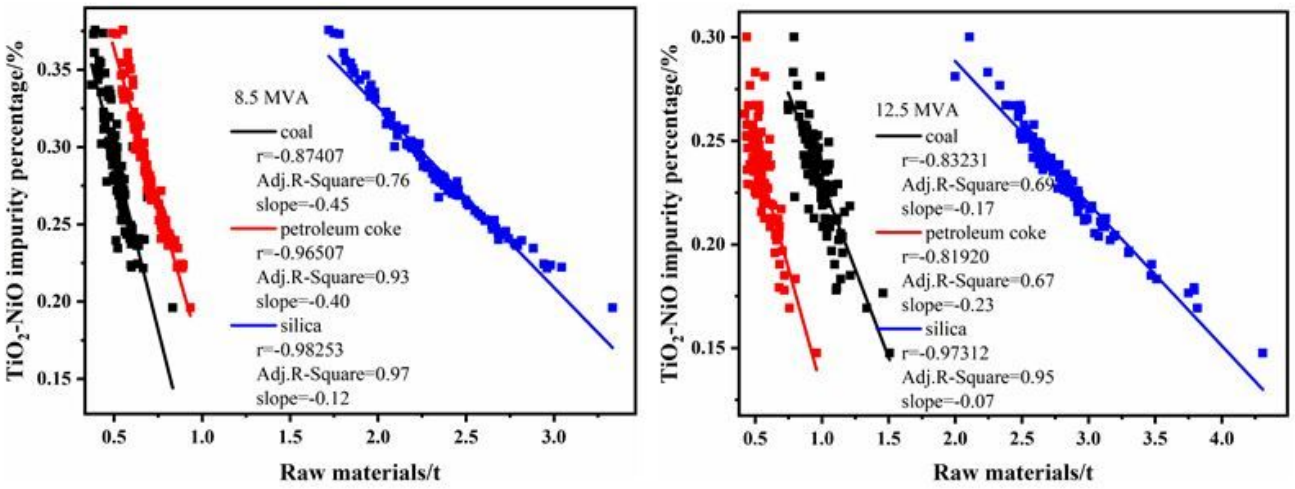

Figure 6

TiO2/NiO impurities in silicon products and total impurities in three raw materials of percent

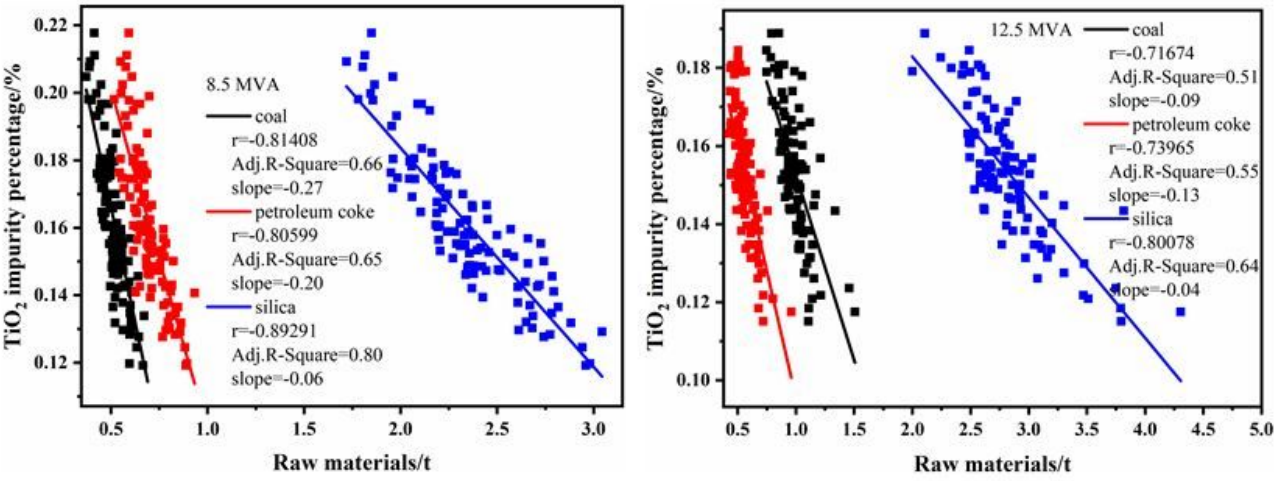

Figure 7

TiO2 impurities in silicon products and total TiO2/NiO impurities in three raw materials of percent

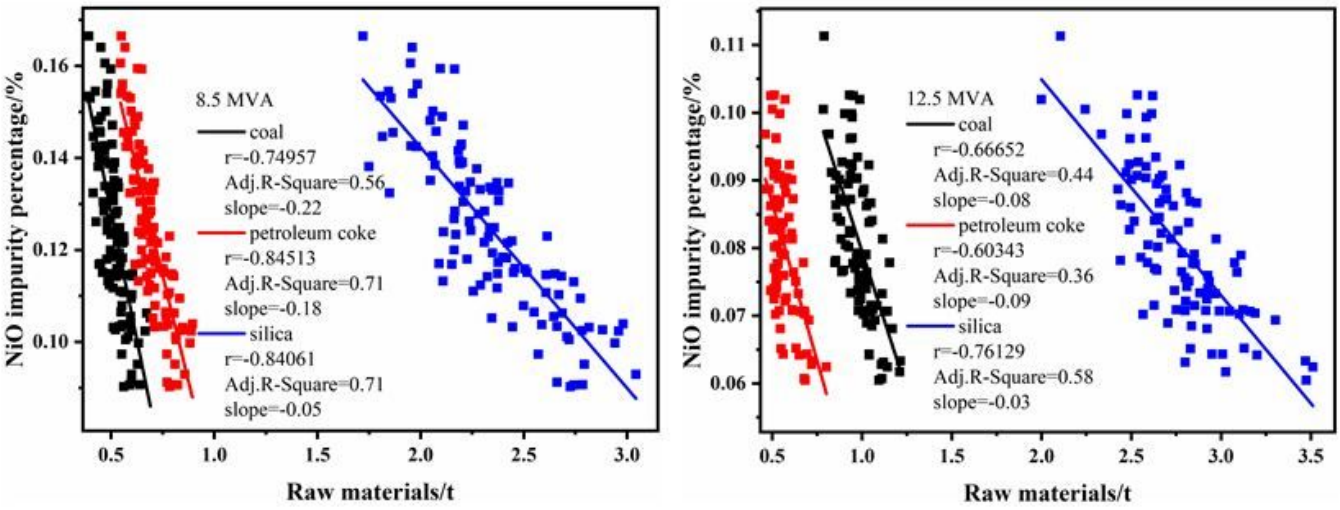

Figure 8

Ni impurities in silicon products and total TiO2/NiO impurities in three raw materials of percent

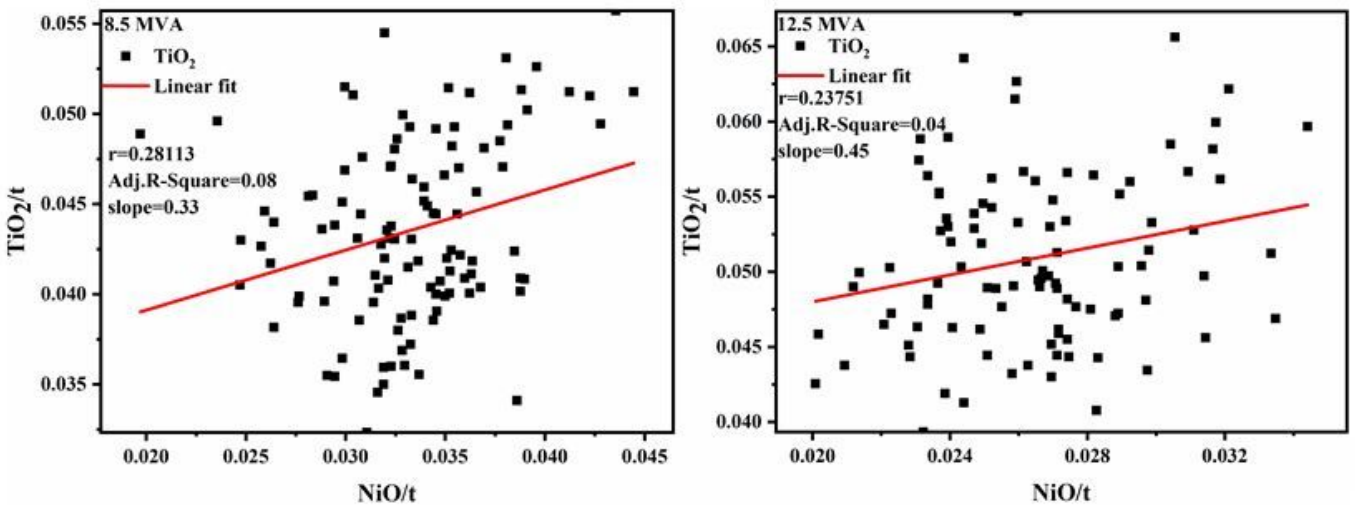

Figure 9

Interaction effect between TiO2 and NiO impurities in silicon

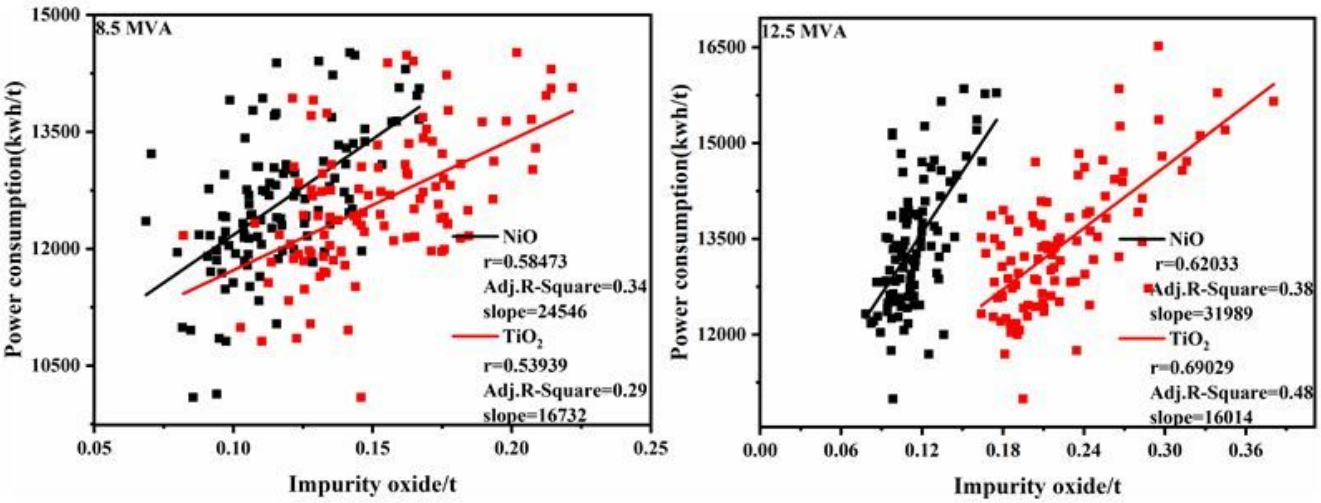

Figure 10

Relationship between Ti and Ni oxides and power consumption

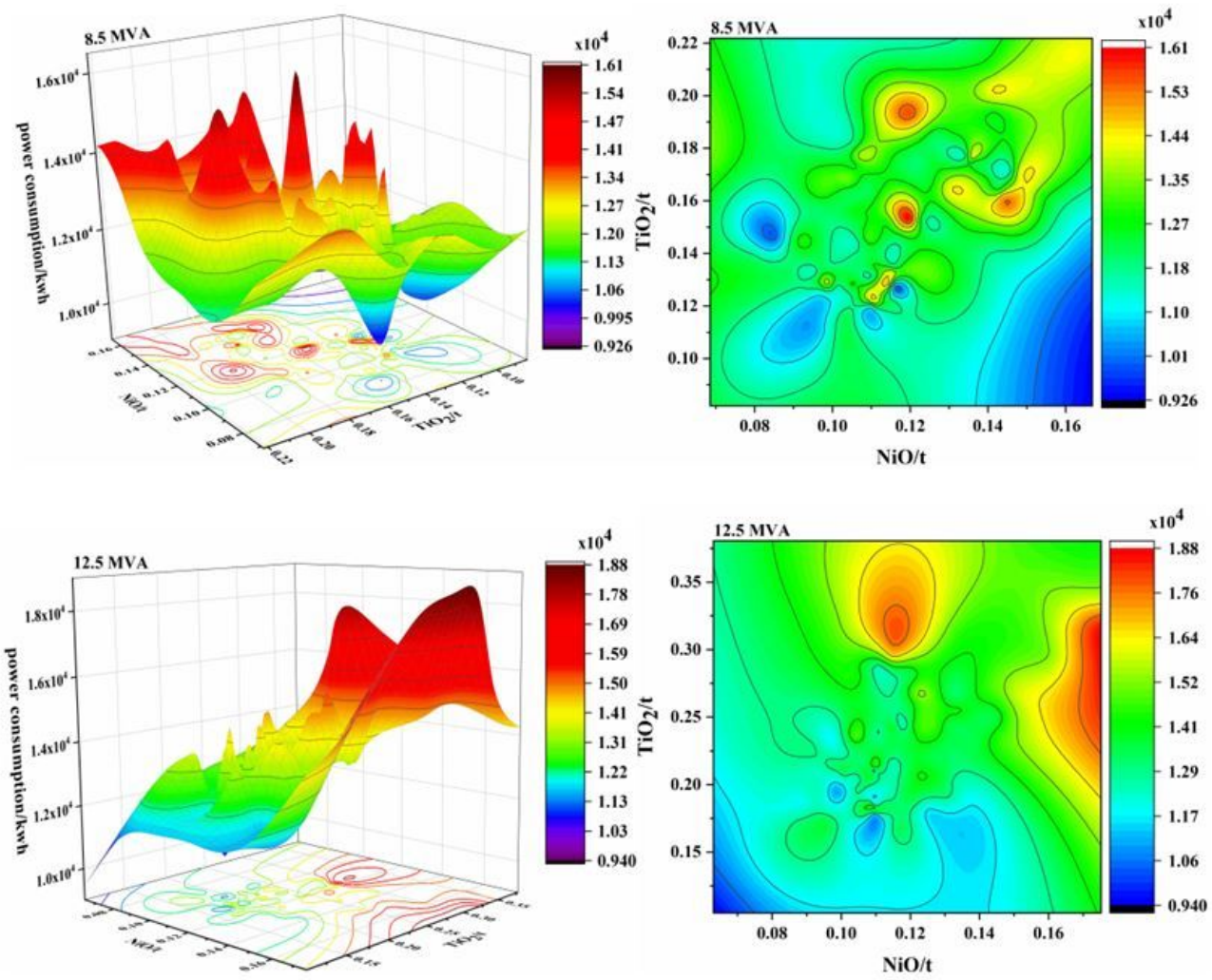

Figure 11

Effect of interaction between TiO2 and NiO impurity oxides on power consumption